

A practical theoretical formalism for atomic multielectron processes: direct multiple ionization by a single Auger decay or by impact of a single electron or photon

Pengfei Liu¹, Jiaolong Zeng^{1,3,†}, and Jianmin Yuan^{1,2,3, a)}

¹⁾*College of Science, National University of Defense Technology, Changsha Hunan 410073, P. R. China*

²⁾*Graduate school of China Academy of engineering Physics, Beijing 100193, P. R. China*

³⁾*IFSA Collaborative Innovation Center, Shanghai Jiao Tong University, Shanghai 200240, P. R. China*

(Dated: 4 February 2022)

Multiple electron processes occur widely in atoms, molecules, clusters, and condensed matters when they are interacting with energetic particles or intense laser fields. Direct multielectron processes are the most involved among the general multiple electron processes and are the most difficult to describe theoretically. In this work, a unified and accurate theoretical formalism is proposed on the direct multielectron processes of atoms including the multiple Auger decay and multiple ionization by an impact of an energetic electron or a photon based on the atomic collision theory described by a correlated many-body Green's function. Such a practical treatment is made possible due to different coherence features of the particles (matter waves) in the initial and final states. We first explain how the coherence characteristics of the ejected continuum electrons is largely destructed, by taking the electron impact direct double ionization process as an example. This process is completely different from the single ionization where the complete interference can be maintained. The detailed expressions are obtained for the energy correlations among the continuum electrons and energy resolved differential and integral cross sections according to the separation of knock-out and shake-off mechanisms for the electron impact direct double ionization, direct double and triple Auger decay, and double and triple photoionization processes. Extension to higher-order direct multielectron processes than triple ionization is straight forward by adding contributions of following knock-out and shake-off processes. The approach is applied to investigate the electron impact double ionization processes of C^+ , N^+ , and O^+ , the direct double and triple Auger decay of the K-shell excited states of C^+ $1s2s^22p^2$ 2D and 2P , and the double and triple photoionization of lithium. Comparisons with available experimental and theoretical results show that our proposed theoretical formalism is accurate and effective in treating the atomic multielectron processes.

I. INTRODUCTION

Multielectron processes occurring in a single Auger decay and in collision of atoms (including atomic ions), molecules, clusters, and condensed matters with a single photon or a single charged particle belong to one of the most interesting areas of physics. They are vital to understand the nature of many-electron and many-particle transitions and play a significant role in a variety of practical applications such as modeling of plasma processes, astrophysics and charge state distribution and evolution of atoms exposed to an electron beam¹ or a radiation field. Multielectron processes can be classified as direct and indirect ones, where multiple electrons are emitted simultaneously or sequentially. The indirect processes are

^{a)}Electronic mail: jlzeng@nudt.edu.cn

determined by removal of an inner-shell electron and subsequent autoionization, where only single electron transitions are involved in each step. Direct processes, however, require sophisticated theoretical methods which should come out of the framework of one-electron approximation.

The correlated motion of electrons in the direct multielectron processes (DMEP) has been a concern of physics since the early days of quantum mechanics². Double photoionization (DPI)³⁻⁷, electron impact double ionization (EIDI)⁸⁻¹⁴ and double Auger decay (DAD)¹⁵⁻¹⁸ are the lowest order of such processes, where two electrons are simultaneously ejected into the continuum state by impact of a single photon or a single electron or by a single Auger decay. A wealth of information on the physical mechanisms, angular distributions and energy correlations between the ejected electrons has provided deeper insight into these electron-electron interaction dynamical processes. Understanding the correlation can help to control the multielectron processes¹⁹. The latest attractive research is the direct triple processes as demonstrated theoretically by Colgan *et al.*^{20,21} for triple photoionization and by Müller *et al.*^{22,23} for triple Auger decay, the authors of the latter work experimentally observed unambiguously a four-electron Auger decay with simultaneous emission of three electrons.

Theoretical description on these correlated multielectron processes, however, poses a formidable challenge to the theorists, even for the simplest test cases of the three-body Coulomb problems of small systems such as the helium atom or the hydrogen molecules^{2,24}. Nearly exact calculations for such systems are available only for bound states, whereas the correlated motion of electrons in DMEP is still not fully understood. A number of sophisticated calculations have been performed for DPI²⁵⁻³⁰, EIDI³¹⁻³⁶ and DAD³⁷⁻³⁹. These theoretical calculations investigated the many-fold differential or integral cross sections by numerically solving the time-dependent Schrödinger equation or by treating the electron-electron interaction as a perturbation to investigate the double continuum process. Most of the calculations deal with the simpler systems such as helium atom and hydrogen molecule, and only a few on Li- and Be-like atoms or atomic ions. For more complex multi-electron atoms, however, such sophisticated calculations are difficult or untractable even for the double continuum process, let alone for the triple and higher order multielectron processes.

As is well known, the electron correlation is a prerequisite for a DMEP to occur, i.e., the highly correlated initial state wave-function and correlated motion in the final state with the exchange of energy between the outgoing electrons. However, the features of electron correlation in the final state are different from that of the initial state in that the first ejected continuum electron is coupled with the remaining environment by the Coulomb interaction, which results in the loss of partial information of the wave phases⁴. By fully taking advantage of the different correlation features, the theoretical description can be greatly simplified with little loss of computation accuracy. The central physical thought is that the interference between different channels (see Fig. 1 for such a pathway, taking a direct quadruple ionization as an example) is largely destructed due to the continuous variations of wave phases in the transition matrix elements. The more ejected electrons, the less the interference effects remain.

In this work, we proposed a practical and accurate theoretical formalism on the DMEPs including multiple Auger decay and multiple ionization by impact of a single photon or electron. Detailed expressions have been obtained for the energy resolved differential and integral cross sections for the direct double and triple processes. The calculations of the fully (angular) differential cross section can also be implemented according to the separation of ionization mechanism. Theoretical treatment for the higher order DMEP than triple processes is even more challenging. To the best of our knowledge, no report on such processes is available in the literature. However, extension of our theoretical formalism to such higher order multiple ionization processes is straight forward. Moreover, most past theoretical investigations on multiple ionization have dealt with simple atomic systems of few electrons such as helium and lithium. Yet our solution can treat any complex heavy Z atoms with many electrons.

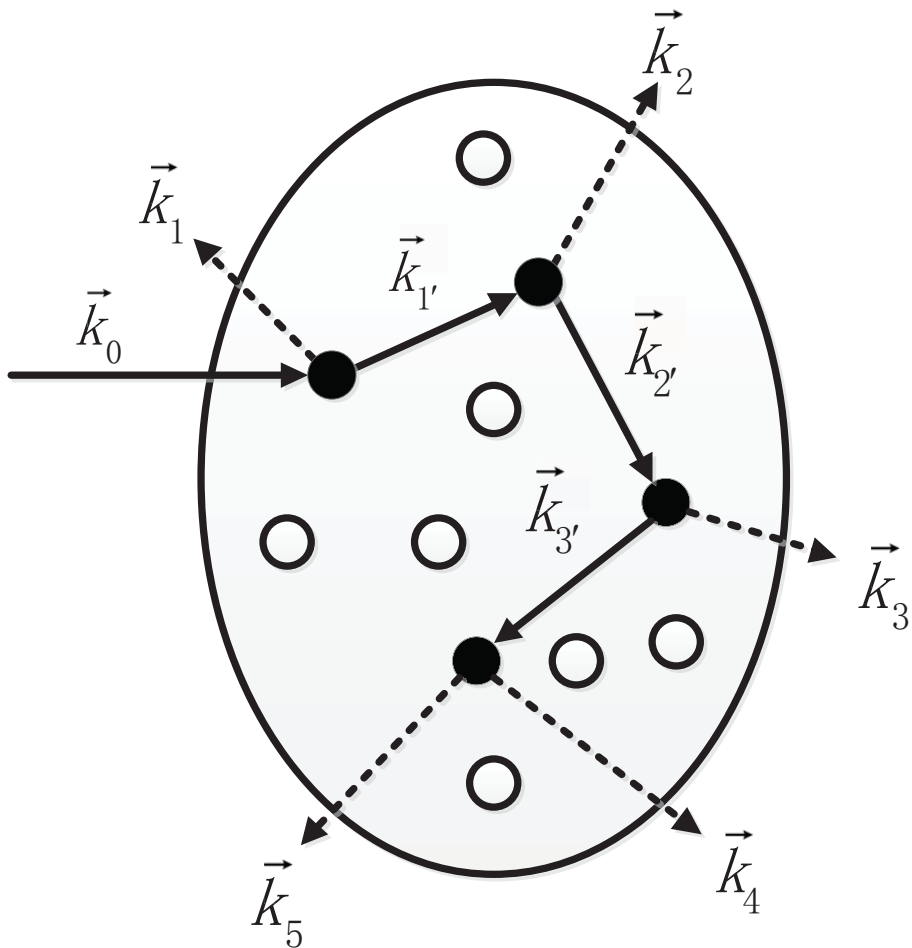


FIG. 1. A schematic illustration of a channel in the atomic direct multielectron processes, taking a quadruple ionization as an example. The momentum of incoming projectile is denoted as \vec{k}_0 and each circle represents a possible electronic state. Along with the pathway, all solid circles constitute a reaction channel. Any solid circles can be replaced by open circles to form another channel.

II. THEORETICAL FORMALISM

First we take the electron impact direct double ionization [also called (e,3e)] processes of an isolated many-electron atom as an example to start our discussion. The complete dynamics, which is described by eight-fold differential cross section (DCS), is spanned over the momentum space of the three continuum electrons where eight independent variables are required considering the energy conservation relation⁴⁰

$$\frac{d\sigma_{if}(E_0, E_1, E_2, \Omega_1, \Omega_2, \Omega_3)}{dE_1 dE_2 d\Omega_1 d\Omega_2 d\Omega_3} = (2\pi)^4 \mu^2 \frac{k_1 k_2 k_3}{k_0} |T_{if}|^2 \quad (1)$$

where i and f represent the initial and final states, k_0 and E_0 the momentum and kinetic energy of the incident electron, E_p , k_p , and Ω_p ($p=1, 2, 3$) the kinetic energy, magnitude of momentum, and solid angle of the three outgoing electrons, and μ the reduced mass of the incident electron and the target. The transition probability amplitude T_{if} , which defines a

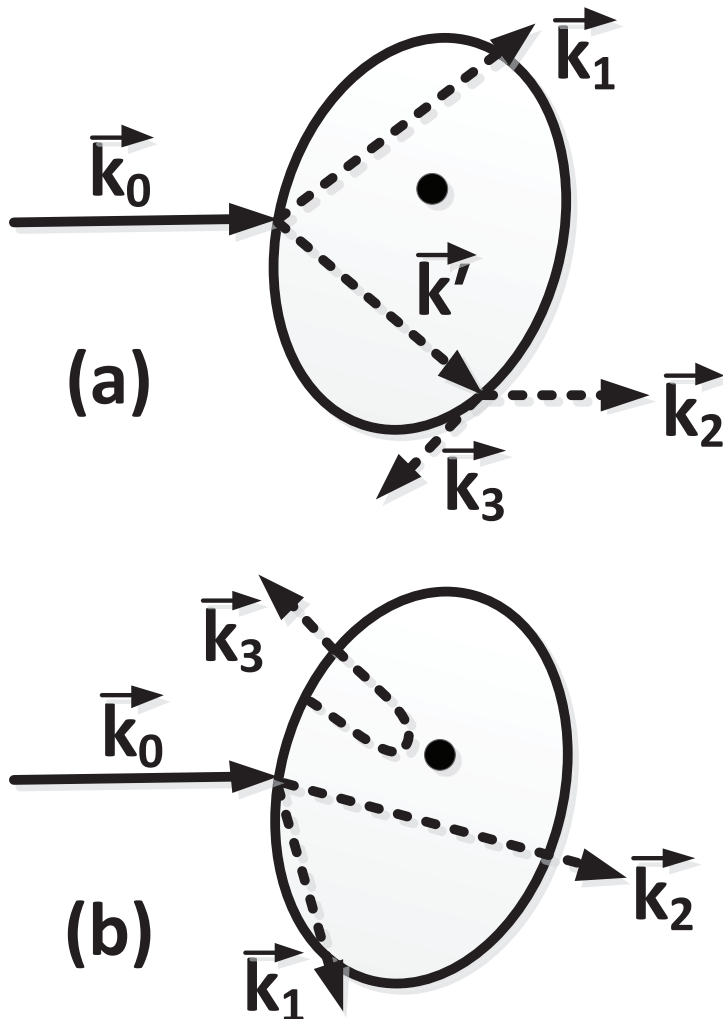


FIG. 2. A schematic representation of the mechanisms of (a) knock-out (KO) and (b) shake-off (SO) in electron impact direct double ionization processes. The momentum vector of the incoming projectile is denoted by an arrow labeled by \vec{k}_0 , and the momenta of the three ejected electrons are denoted by \vec{k}_1 , \vec{k}_2 , and \vec{k}_3 . The nuclei of the atom is shown as a full dot.

Lippmann-Schwinger equation for the transition matrix element, can be expressed in terms of the Green's function

$$T_{if} = \langle \vec{k}_1, \vec{k}_2, \vec{k}_3, \varphi_f | V_f (1 + G^+ V_i) | \vec{k}_0, \psi_i \rangle \quad (2)$$

where $|\vec{k}_0, \psi_i \rangle (V_i)$ and $|\vec{k}_1, \vec{k}_2, \vec{k}_3, \varphi_f \rangle (V_f)$ are the initial and final state vectors (transition potential operators), G^+ the fully correlated four-body Green's function, which is the resolvent of the whole physical system of incident electron plus target with appropriate boundary conditions. The state vectors satisfy the time-independent Schrödinger (or relativistic quantum mechanics) equation $H_i |\vec{k}_0, \psi_i \rangle = E_i |\vec{k}_0, \psi_i \rangle$ and $H_f |\vec{k}_1, \vec{k}_2, \vec{k}_3, \varphi_f \rangle = E_f |\vec{k}_1, \vec{k}_2, \vec{k}_3, \varphi_f \rangle$

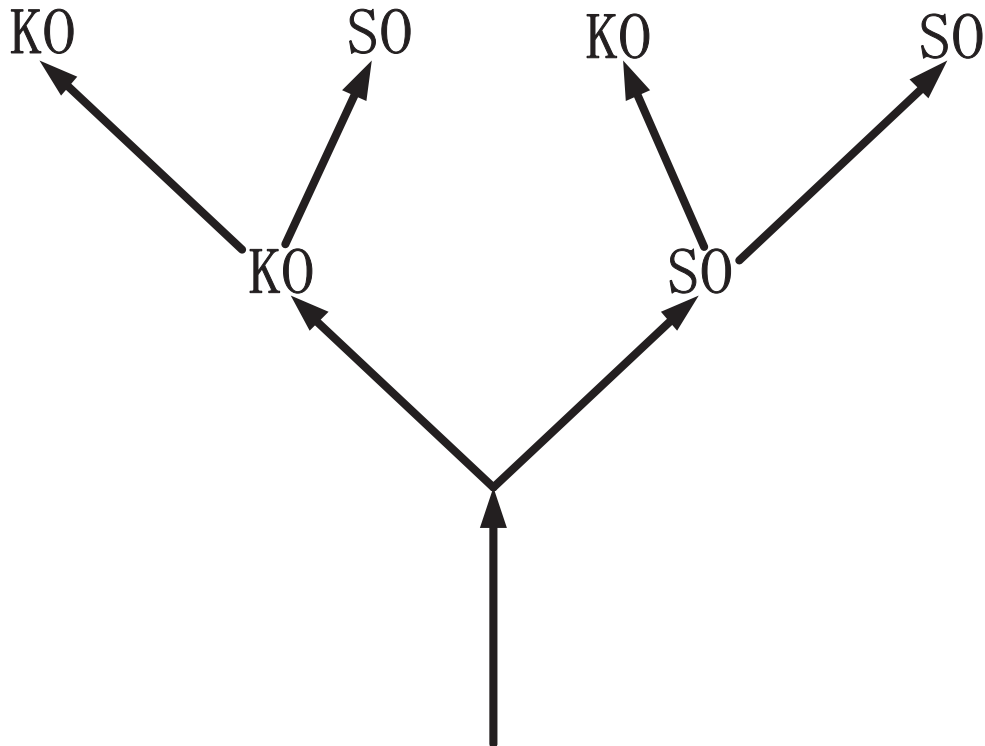


FIG. 3. A schematic diagram of the physical mechanisms following the KO and SO processes of the DDAD in the DTAD. It is straight forward to extend it to higher order multielectron processes.

$E_f |\vec{k}_1, \vec{k}_2, \vec{k}_3, \varphi_f \rangle$ with H_i and H_f being the Hamiltonians of the initial projectile-atom system and of the three charged continuum electrons in the field of a doubly charged ion and E_i and E_f the energies of the initial and final state. In the description of final state, the designation of electron 1, 2, and 3 is introduced for convenience, yet there is no other special meaning as these electrons are ejected simultaneously in the direct ionization processes. In both the initial and final wave functions, the effects of all potentials including the exchange interaction potential are included in the calculations and hence they should be treated in the same footing. The exchange potential operators V_i and V_f describe the Coulomb interaction between the incident electron and the target before collision and between the three outgoing electrons and the final state φ_f after collision. Assuming non-interacting asymptotic states after collision V_f can be expressed as

$$V_f = V_{e_1 e_2} + V_{e_1 e_3} + V_{e_2 e_3} + V_{e_1 f} + V_{e_2 f} + V_{e_3 f} \quad (3)$$

Considering the intermediate states after single ionization [see Fig. 2(a)], all bound states and continuum states of the projectile-target system form a complete set and thus satisfy the closure condition

$$\sum_n \int_{\vec{k}'} d\vec{k}' |\vec{k}_1, \vec{k}', \chi_n \rangle \langle \vec{k}_1, \vec{k}', \chi_n| = 1 \quad (4)$$

where $|\chi_n \rangle$ is a (quasi-)bound state of the intermediate ion with one higher charge. In the above equation, we number one of the continuum electron as "1" for the convenience of expression. As we pointed out in the above that the simultaneously ejected electrons

are indistinguishable and thus the designation of electron "1" has no special role. The summations over the intermediate middle states include a summation over all possible bound states of the target and a summation and integration over a complete set of bound and continuum states of one more highly ionized target. Inserting this identity into the probability amplitude T_{if} one obtains

$$T_{if} = \sum_n \int_{\vec{k}'} \langle \vec{k}_1, \vec{k}_2, \vec{k}_3, \varphi_f | V_f | \vec{k}_1, \vec{k}', \chi_n \rangle d\vec{k}' \langle \vec{k}_1, \vec{k}', \chi_n | (1 + G^+ V_i) | \vec{k}_0, \psi_i \rangle \quad (5)$$

Let us denote $\langle \vec{k}_1, \vec{k}_2, \vec{k}_3, \varphi_f | V_f | \vec{k}_1, \vec{k}', \chi_n \rangle = a(\vec{k}') e^{i\phi_a(\vec{k}')}$ and $\langle \vec{k}_1, \vec{k}', \chi_n | (1 + G^+ V_i) | \vec{k}_0, \psi_i \rangle = b(\vec{k}') e^{i\phi_b(\vec{k}')}$, where $a(\vec{k}')$ and $b(\vec{k}')$ represent the absolute magnitudes of the respective matrix element and $\phi_a(\vec{k}')$ and $\phi_b(\vec{k}')$ denote their phases. For a particular final state of $|\vec{k}_1, \vec{k}_2, \vec{k}_3, \varphi_f \rangle$, $\phi_a(\vec{k}')$ and $\phi_b(\vec{k}')$ vary with \vec{k}' continuously from the lowest to the highest possible values and therefore the interference between different channels denoted by \vec{k}' is largely destructed by the integrations over \vec{k}' when we calculate the cross section between the initial and final states. The possible nonzero interference would very highly sensitively depend on some particular values of \vec{k}_1 , \vec{k}_2 , and \vec{k}_3 , and the integrations over the directions of \vec{k}_2 and \vec{k}_3 will average out the existing interference effects when we calculate the energy correlated differential cross sections or the total cross sections. The last possibility of the missing of interference effects is the insufficient high enough angular resolution of the momenta \vec{k}_2 and \vec{k}_3 measurement even for a complete momentum differential cross section. As we know, the high sensitivity on particular values of momenta of three continuum electrons requires a very high resolution in the experiment, which is perhaps beyond the capability of our most advanced instrument or is limited by the physical principle.

It is also helpful to express the probability amplitude [Eq. (2)] as a multiple scattering series, which can be derived by iterating the integral Lippmann-Schwinger equation of the Green operators⁴⁰. If we consider only the second order terms, the dominant mechanisms of shake-off (SO) and knock-out (KO) [which is sometimes called two step 2 and two step 1 in the literature] can be identified. KO describes the correlated dynamics of the three continuum electrons, where the incident electron ionizes a secondary electron and then either one knocks out the third electron in an inelastic scattering process. A removal of the second electron causes a sudden change of atomic potential and a third electron can be shaken off to the continuum state, which is called SO mechanism. In the multiple scattering series, there are many terms which can be categorized into the mechanisms of either KO [see Fig. 2(a)] or SO [see Fig. 2(b)]. According to the separation of KO and SO mechanisms, the angular differential cross sections can be obtained. After integrating the eight-fold DCS over the solid angles of all electrons, two-fold DCS based on the two mechanisms reads

$$\frac{d\sigma_{if}^{KO}(E_0, E_1, E_2)}{dE_1 dE_2} = \frac{1}{\pi} \sum_n \frac{d\sigma_{in}(E_0, E_1)}{dE_1} \frac{d\sigma_{nf}(E_1, E_2)}{dE_2} \quad (6)$$

$$\frac{d\sigma_{if}^{SO}(E_0, E_1, E_2)}{dE_1 dE_2} = \frac{1}{\pi} \sum_n \frac{d\sigma_{in}(E_0, E_1)}{dE_1} | \langle E_2, E_1 - I_n - E_2, \varphi_f | E_1, \chi_n \rangle |^2 \quad (7)$$

where I_n is the ionization energy of state $|\chi_n \rangle$, $\frac{d\sigma_{in}(E_0, E_1)}{dE_1}$ and $\frac{d\sigma_{nf}(E_1, E_2)}{dE_2}$ are, respectively, the electron-impact single ionization DCS from $|\psi_i \rangle$ to intermediate state $|\chi_n \rangle$ and from $|\chi_n \rangle$ to the final state $|\varphi_f \rangle$. The integral cross section can be obtained by integrating over the kinetic energies of continuum electrons

$$\sigma_{if}^{KO}(E_0) = \frac{1}{2\pi} \sum_n \sigma_{in}(E_0) \int_0^{E_0 - I_i} f(E_0, E_1) \sigma_{nf}(E_1) dE_1 \quad (8)$$

$$\sigma_{if}^{SO}(E_0) = \frac{1}{2\pi} \sum_n \sigma_{in}(E_0) \int_0^{E_0-I_i} dE_1 f(E_0, E_1) \int_0^{E_0-I_i-I_n} | \langle E_2, E_1-I_n-E_2, \varphi_f | E_1, \chi_n \rangle |^2 dE_2 \quad (9)$$

where I_i and I_n being the ionization potentials of states $|\psi_i\rangle$ and $|\chi_n\rangle$. A factor of $\frac{1}{2}$ is introduced to avoid double counting of the contribution. The function $f(E_0, E_1)$ describes the population fraction per unit energy interval of E_1 in the second collision, which is defined as $\frac{d\sigma_{in}(E_0, E_1)}{dE_1} = \sigma_{in}(E_0) f(E_0, E_1)$.

The above formulas of KO and SO mechanisms are readily applicable to the DPI and DAD processes by letting $f(E_0, E_1) = 1$ and replacing the electron impact ionization cross section $\sigma_{in}(E_0)$ (the first term in the right hand) by the single photoionization cross section or single Auger decay rate, respectively. For example, the DAD rates due to KO and SO mechanisms reads as

$$A_{if}^2(KO) = \frac{1}{\pi} \sum_n A_{in}^1 \sigma_{nf}(E_0) \quad (10)$$

$$A_{if}^2(SO) = \frac{1}{\pi} \sum_n A_{in}^1 \int_0^{E_0-I_i} | \langle E_1, E_0 - I_n - E_1, \varphi_f | E_0, \chi_n \rangle |^2 dE_1 \quad (11)$$

where A_{in}^1 is the single Auger decay rate from the initial state $|\psi_i\rangle$ to a middle state $|\chi_n\rangle$. Note, however, that for the DPI process the electron impact cross section in the second step of KO should include only those contributions which fulfill the dipole selection rule. Past work showed that the separate formulation of KO and SO mechanisms offers an accurate description for the DPI^{5,41-44} and DAD^{37,45-47}. The separability of the two-step expressions in the KO and SO indicates that the ejected continuum electrons are not as highly correlated as the bound electrons in the initial state. The Coulomb interaction with the second electron and remaining atomic ion modifies the matter wave phases of the first electron and thus induces the loss of partial phase information. This is a common phenomenon for the direct multi-electron processes and hence a unified theoretical description is feasible. The unified theory bridges these direct multiple processes and reveals such connections. It also offers a deeper insight into the similarity between these physical processes, which has been demonstrated between the DPI and electron impact single ionization processes^{10,43}. Further experimental and theoretical work should be able to demonstrate the similarity between the Auger decay and ionization processes by a single photon or a single electron.

The above method can readily be extended to the higher order multielectron processes. Take the direct triple Auger decay (DTAD) process as an example to illustrate the procedure. According to the separation of physical mechanisms, DTAD can proceed via the two routes of KO and SO which results in four pathways (see Fig. 3). Following the KO mechanism of DAD, there are also two pathways of KO and SO with the decay rate being expressed as

$$A_{if}^3(KO + KO) = \frac{1}{2\pi^2} \sum_j \sum_n A_{ij}^1 \sigma_{jn}(E_0) \int_0^{E_0-I_j} f(E_0, E_1) \sigma_{nf}(E_1) dE_1 \quad (12)$$

$$A_{if}^3(KO+SO) = \frac{1}{2\pi^2} \sum_j \sum_n A_{ij}^1 \sigma_{jn}(E_0) \int_0^{E_0-I_j} dE_1 f(E_0, E_1) \int_0^{E_0-I_j-I_n} | \langle E_2, E_1-I_n-E_2, \varphi_f | E_1, \chi_n \rangle |^2 dE_2 \quad (13)$$

Comparing with the KO mechanism in the DAD, we term these two processes as a double KO (KO+KO) and a KO and SO (KO+SO). The corresponding expressions following the SO can be similarly obtained, which results in the mechanisms of what are termed as a double SO (SO+SO) and SO+KO

$$A_{if}^3(SO + KO) = \frac{1}{2\pi^2} \sum_j \sum_n A_{ij}^1 \int_0^{E_0 - I_j} dE_1 | \langle E_1, E_0 - I_j - E_1, \varphi_n | E_0, \psi_j \rangle |^2 \sigma_{nf}(E_1) \quad (14)$$

$$A_{if}^3(SO+SO) = \frac{1}{2\pi^2} \sum_j \sum_n A_{ij}^1 \int_0^{E_0 - I_j} dE_1 | \langle E_1, E_0 - I_j - E_1, \varphi_n | E_0, \psi_j \rangle |^2 \int_0^{E_0 - I_j - I_n} | \langle E_2, E_1 - I_n - E_2, \varphi_f | E_1, \chi_n \rangle |^2 \quad (15)$$

The above four formulas of DTAD are also applicable for the direct triple photoionization by replacing the single Auger decay rate A_{ij}^1 (the first term in the right hand) by the single photoionization cross section.

The required quantities including the single Auger decay rate, electron- and photon-impact single ionization cross section are obtained using the Flexible Atomic Code developed by Gu⁴⁸ and the R-matrix method⁴⁹⁻⁵². The theory on these single electron processes can be found elsewhere^{45-47,50-55} and therefore the details are not given here. To obtain as accurate results as possible, electron correlations should be adequately considered in each step^{56,57}.

Here we do not give the expressions of higher order multi-electron processes such as direct tetrad Auger decay, electron impact direct triple ionization and tetrad photoionization, yet extension of the approach to these processes are straight forward. It should also be extendable to more complex physical systems such as molecules and clusters. The present theoretical formalism is helpful to understand other particle-particle many-body scattering problem⁵⁸ and long-range interactions between ultracold atoms and molecules⁵⁹.

III. RESULTS AND DISCUSSIONS

In what follows, we apply the unified theoretical formalism to investigate three typical multielectron processes of multiple Auger decay and multiple ionization by impact of a single photon or a single electron with atoms or atomic ions. First we deal with the electron impact double ionization processes.

A. Electron impact double ionization

Atomic helium and helium-like ions are the simplest systems to investigate the electron impact double ionization processes^{14,60,61}. For such simple systems, only direct processes are possible. Time-dependent close-coupling (TDCC) method has been applied to these systems⁶²⁻⁶⁵, which have provided a good description for the double ionization cross sections. Here we deal with more complex systems of C^+ , N^+ , O^+ , which still lack accurate theoretical explanations for the measured experimental results⁶⁶⁻⁶⁸. For these ions, no close-coupling calculations have been carried out up to now. Recently, Jonauskas *et al.*⁶⁹ investigated the electron impact double ionization cross section of C^+ and O^+ by presenting the process as a sequence of two- and three-step processes arising from ionization-ionization, ionization-excitation-ionization, and excitation-ionization-ionization processes.

First we investigate the energy resolved double DCS which reflects the energy correlations in the electron impact direct double ionization. Figure 4 shows the double DCS for a pathway of $e+C^+ 1s^2 2s^2 2p^2 P^o \rightarrow C^{2+} 1s^2 2s^2 {}^1S + 2e \rightarrow C^{3+} 1s^2 2s^2 S + 3e$ at the incident electron energy of 82.36, 112.36 and 232.36 eV, which are above the double ionization threshold by 10.0, 40.0, and 160.0 eV, respectively. The single and double ionization potentials of C^+ were calculated to be 24.96 and 72.36 eV, which is in good agreement with the experimental values⁷⁰ of 24.38 and 72.27 eV (see table 1). The theoretical DCS is a summation over the mechanisms of both KO and SO. At lower incident electron energy

TABLE I. Single and double ionization potentials (IP) and 1s single IP (in units of eV) of the ground terms of C⁺, N⁺, and O⁺ and comparison with the experiment⁷⁰.

Ions	Ground term	Single IP		Double IP		1s IP
		This work	NIST ⁷⁰	This work	NIST ⁷⁰	
C ⁺	1s ² 2s ² 2p ² ² P ^o	24.96	24.38	72.36	72.27	314.55
N ⁺	1s ² 2s ² 2p ² ³ P	30.08	29.60	76.94	77.05	433.07
O ⁺	1s ² 2s ² 2p ³ ⁴ S ^o	35.13	35.12	88.30	90.06	565.77

(Fig. 4(a), 10.0 eV above double ionization threshold), three continuum electrons tend to share the available energy nearly equivalently. With increasing incident electron energy, however, one of the three electrons tend to possess most of the available energy with a large probability, which results in two slower electrons in the process. The higher energy of the incident electron, the larger probability of the fast electron. The maximal double DCS decreases with increasing incident electron energy. Similar conclusion can be drawn for all other channels. To save space, the double DCS of N⁺ and O⁺ are not given here.

In Fig. 5 we compare the electron impact double ionization integral cross sections for the ground term of C⁺ with the experimental⁶⁶⁻⁶⁸ as well as other theoretical results⁶⁹. From the inspection of this figure, there is an excellent agreement between our theory and the most recent experimental results obtained by Lecointre *et al.*⁶⁸ from the double ionization threshold to an incident electron energy of 200 eV. In the intermediate energy range of 200-500 eV, the experimental cross section is a little larger than our theoretical prediction. With the further increase of incident electron energy, we found again a good agreement between the theoretical and experimental results. Compared with the earlier measurement of Zambra *et al.*⁶⁶, however, a reasonable agreement is found only at the incident electron energy range 300-500 eV. In particular, the shape and magnitude near the peak cross section is completely different. Lecointre *et al.*⁶⁸ measured two peak values of cross section at ~ 160 and ~ 900 eV, while Zambra *et al.*⁶⁶ measured only one peak value at ~ 700 eV. The only available theoretical work available in the literature obtained by Jonauskas *et al.*⁶⁹ predicted a larger peak cross section than our calculation and all available experimental measurements⁶⁶⁻⁶⁸. A large discrepancy can also found near the ionization threshold for the total double ionization cross section obtained by Jonauskas *et al.*⁶⁹.

To have a better understanding of this double ionization process, we give in Fig. 5 the respective contributions of different mechanisms including the direct and indirect processes. The direct double ionization refers to contributions of the mechanisms of KO and SO and indirect processes include sequential double ionization (electron impact single ionization of 1s and subsequently autoionization) and electron impact excitation of 1s and then double autoionization. Obviously, the cross sections are dominated by the KO mechanisms of direct double ionization from the double ionization threshold up to ~ 300 eV, which is perfectly predicted by our theoretical approach. With increasing incident electron energy up to ~ 315 eV, the 1s ionization channels are opened and the indirect ionization processes begin to play a role. Above ~ 430 eV, the cross section contributed by the indirect processes becomes larger than that of direct double ionization channels. On the other hand, the cross section contributed by the KO mechanism decreases more evidently than SO with increasing incident electron energy until the latter becomes larger than the former at a very high incident electron energy.

In Figs. 6 and 7 we compare the theoretical electron impact double ionization integral cross sections of the ground term of N⁺ and O⁺ with the experimental results^{66,68}. The single and double ionization potentials of these two ions are listed in table 1 along with the experimental values⁷⁰. The contributions to the cross section from different mechanisms including the direct and indirect processes are given to evaluate their respective importance. For O⁺, theoretical results obtained by Jonauskas *et al.*⁶⁹ are also given. For both ions, there is a general good agreement between our theoretical cross sections and the most recent experimental results of Lecointre *et al.*⁶⁸, yet a large discrepancy is found with the earlier measurement of Zambra *et al.*⁶⁶. Near ionization threshold, the cross sections are

TABLE II. Auger decay rates (s^{-1}) of the dominant pathways for the SAD (A^1), DDAD (A^2), and DTAD (A^3) processes from the initial terms of C^+ $1s2s^22p^2\ ^2D$ and $\ ^2P$. The intermediate terms of C^{2+} and C^{3+} are given to specify the pathways. Figures in brackets indicate powers of ten.

Initial C^+	C^{2+}	A^1	C^{3+}	A^2	Final C^{4+}	A^3
$1s2s^22p^2\ ^2D$	$1s^22s^2\ ^1S$	5.026[13]	$1s^22s\ ^2S$	1.388[12]	$1s^2$	4.086[9]
	$1s^22s2p\ ^3P^o$	7.641[12]	$1s^22s\ ^2S$	1.620[11]	$1s^2$	5.288[8]
	$1s^22s2p\ ^3P^o$		$1s^22p\ ^2P^o$	1.099[11]	$1s^2$	4.872[8]
	$1s^22s2p\ ^1P^o$	3.546[13]	$1s^22s\ ^2S$	7.360[11]	$1s^2$	2.412[9]
	$1s^22s2p\ ^1P^o$		$1s^22p\ ^2P^o$	5.528[11]	$1s^2$	2.385[9]
	$1s^22s^02p^2\ ^1D$	5.526[13]	$1s^22s\ ^2S$	1.903[11]	$1s^2$	6.365[8]
	$1s^22s^02p^2\ ^1D$		$1s^22p\ ^2P^o$	2.288[12]	$1s^2$	9.405[9]
	total	1.557[14]	total	5.762[12]	total	2.168[10]
$1s2s^22p^2\ ^2P$	$1s^22s2p\ ^1P^o$	1.216[13]	$1s^22s\ ^2S$	2.530[11]	$1s^2$	8.534[8]
	$1s^22s2p\ ^1P^o$		$1s^22p\ ^2P^o$	1.896[11]	$1s^2$	8.088[8]
	$1s^22s^02p^2\ ^3P$	5.606[13]	$1s^22p\ ^2P^o$	2.399[12]	$1s^2$	9.993[9]
	total	7.670[13]	total	3.102[12]	total	1.194[10]

dominated by the KO mechanisms of direct double ionization, while SO gradually plays a role with increasing incident energy. Jonauskas *et al.*⁶⁹ overestimated the double ionization cross section around the peak value and their theoretical double ionization threshold is also larger than the experimental value. Our results represent the best understanding on the electron impact double ionization of C^+ , N^+ and O^+ . The contributions from various direct and indirect double ionization mechanisms are identified for the first time.

It is interesting to have a comparison of the cross sections of the three ions of C^+ , N^+ and O^+ . Although these ions differ by one more electron from each other, there is a large difference for their integral cross sections. At lower incident electron energy near the threshold, the peak cross section increases from 3.9 Mb for C^+ to 6.5 Mb for N^+ and to 10.8 Mb for O^+ , which are dominantly contributed by the KO mechanism of direct double ionization. However, the cross sections contributed by the indirect processes decreases fast with the increase of atomic number from C^+ to O^+ .

B. Double and triple Auger decay

Next we apply our developed theory to investigate the direct double and triple Auger decay processes. We take the Auger decay of the K-shell excited states $1s2s^22p^2\ ^2D$ and $\ ^2P$ of C^+ as examples to illustrate the effectiveness of the approach. The direct double and triple Auger decay of these autoionization states have been experimentally observed through measuring the single, double and triple photoionization cross section by Müller *et al.*²² and theoretically investigated by Zhou *et al.*⁷¹. In table 2 we give the decay rates of the dominant pathways for the single Auger decay (SAD), DDAD and DTAD of $1s2s^22p^2\ ^2D$ and $\ ^2P$. Through the states of $1s^22s^x2p^y$ ($x + y = 2$) these K-shell excited states decay to $1s^22s^x2p^y$ ($x + y = 1$) of C^{3+} in the DDAD. All these paths result in the production of the ground state $1s^2$ of C^{4+} in the DTAD process. By assuming that the signatures in the double and triple photoionization of the ground term $1s^22s^22p$ of C^+ originate solely from the DDAD and DTAD processes of $1s2s^22p^2\ ^2D$ and $\ ^2P$ terms, the resulting double and triple photoionization cross sections are shown in Fig. 8. A comparison with the experimental data^{22,23} shows that a good agreement is found between the theory and experiment for the single, double, and triple photoionization cross sections. Such a good agreement confirmed that the signatures in the double and triple photoionization observed in the experiment²² are solely due to the DDAD and DTAD of the K-shell states. On the other hand, it also suggests that the interference effects are in general negligible between SO and KO in the DDAD and between the four pathways in the DTAD processes.

To gain more insight into the DTAD process, we have also investigated the energy correlation among the three Auger electrons. Fig. 9 shows the total probability density over a

summation of the four mechanisms as a function of energies of two Auger electrons for the four strongest pathways of $1s2s^22p^2\ ^2D$ (the first, fourth, fifth, and seventh lines in table 2). It is concluded that the DTAD process favors one faster and two slower electrons. The probability density is very small for equal sharing of the energy among the three electrons at a higher photon energy. Fig. 10 shows the probability density for the pathway of $C^+ 1s2s^22p^2\ ^2D \rightarrow C^{2+} 1s^22s^2\ ^1S + e \rightarrow C^{3+} 1s^22s\ ^2S + 2e \rightarrow C^{4+} 1s^2\ ^1S + 3e$ (the first line in table 2) contributed by (a) double KO, (b) KO+SO, (c) SO+KO, and (d) double SO. Among the four mechanisms, double KO dominates the decay processes. The probability density of KO+SO and SO+KO is smaller by more than one order of magnitude and that of double SO is smaller by more than two orders of magnitude than that of double KO.

C. Double and triple photoionization

Most researches on DPI are carried out on atomic helium and helium-like ions (for examples, see^{43,44,72,73} and references therein), which are the simplest systems for such a process to occur. Atomic lithium is a system with only one more electron than helium, yet its theoretical description of DPI is much more complicated^{27,32,74–77}. Various theoretical methods have been developed including convergent close-coupling (CCC)⁷⁶, time-dependent close coupling (TDCC)^{27,74}, R-matrix with pseudostates (RMPSs)⁷⁴ and other theoretical method⁷⁵. Experimentally, Huang *et al.*⁷⁸ and Wehlitz *et al.*⁷⁹ measured the double-to-single ratios of photoionization cross sections of atomic Li. Lithium atom is also the prototype object to investigate the triple photoionization (TPI), both theoretically^{75,80–85} and experimentally⁸⁶. In order to investigate both the DPI and TPI processes, we chose atomic lithium as our study object.

The calculated double-to-single ratio of photoionization cross section of lithium is shown in Fig. 11(a) in a black solid line. The separate contributions from the mechanisms of KO and SO are given in a dashed and dotted line, respectively. It can be seen that only direct ionization processes contributed to the DPI cross section from the ionization threshold to a photon energy of 150.3 eV and it originates predominantly from the KO mechanism. With the increase of photon energy up to 170.1 eV (which corresponds to the opening of channel $h\nu + 1s^22s \rightarrow 2s^2 + e \rightarrow 2s + 2e$), the cross section contributed by SO processes gradually increases and plays a role. At the photon energy of 710.0 eV, the SO and KO mechanisms have an equivalent contribution. With the further increase of photon energy from 710.0 eV, the SO mechanism is becoming more important than KO and it dominates in the direct DPI at a higher photon energy. Obviously, there are additional contribution from the photon energy of 150.3 eV, which can be seen from the rapid increase of the cross section. We have identified that the additional contribution originates from the indirect DPI processes. It is caused by the ionization of $1s$ electron plus excitation of another $1s$, resulting in the production of $1s^0nl n'l'$ excited states. These highly excited states lie above the $1s$ threshold of Li^+ and they decay by Auger processes to the doubly ionized states of Li^{2+} . The most important indirect pathways originate from $1s^02s^2$, $1s^02s2p$ and $1s^02s3s$. The first steep increase of the double-to-single ratio is due to $1s^02s^2$ with a threshold energy of 150.3 eV and to $1s^02s2p$ at a photon energy of 150.5 eV. The second increase located at 163.2 eV originates from the opening of channel $1s^02s3s$.

We compare our theoretical double-to-single ratio of photoionization cross section with the available experimental^{78,79} and theoretical results^{74,76} in the literature. From the inspection of Fig. 11(a), we found an excellent agreement between our theoretical results and both experimental measurements carried out by Wehlitz *et al.*⁷⁹ and Huang *et al.*⁷⁸ in photon energy range from the double ionization threshold to 120 eV. From the photon energy of 120 eV to the opening of indirect channel of $1s^02s^2$, there is also a good agreement with the experiment of Huang *et al.*⁷⁸. To have a better comparison, the double-to-single ratio from the ionization threshold to 140 eV was enlarged in the inset along with available theoretical results obtained by Kheifets *et al.*⁷⁶ (length and velocity gauges of CCC calculations) and Colgan *et al.*⁷⁴ (length gauge of TDCC, length and velocity gauges of RMPS). Obviously, our theoretical results are closer to the experimental values of Wehlitz *et al.*⁷⁹ and Huang

*et al.*⁷⁸ than other theories. At a higher photon energy, our theory agrees reasonably well with the only available experiment of Wehitz *et al.*⁷⁹. The theoretical results obtained by Colgan *et al.*⁷⁴ using a velocity gauge of RMPS underestimated the double-to-single ratio. The underestimation is due to that they did not include the contribution of indirect double ionization processes in their calculations.

The ratio of triple-to-single photoionization cross section is presented in Fig. 11(b) in a solid line. The contributions of KO+KO, KO+SO, SO+KO, and SO+SO mechanisms are represented by a red dashed, blue dotted-dashed, dotted-dotted-dashed, and green dotted line, respectively. At a lower photon energy near the ionization threshold, the largest cross section is contributed by the KO+KO mechanism. With increasing photon energy, the contributions of KO+SO, SO+KO, and SO+SO mechanisms become more and more important. Comparison with the experimental results obtained by Wehitz *et al.*^{82,86} and Juranić *et al.*⁸⁴ shows that a good agreement is found between our theoretical calculations and the latest experimental measurements of Juranić *et al.*⁸⁴. In the inset of Fig. 11(b), we compare our theoretical triple photoionization cross section of the ground state of atomic Li with available theoretical results reported in the literature obtained by Colgan *et al.*²⁷, Emmanouilidou and Rost⁸⁵, and Samson *et al.*⁷² and experimental measurements by Wehitz *et al.*^{82,86} and Juranić *et al.*⁸⁴ in the photon energy range from triple ionization threshold to 600 eV. Our results are in a good agreement with the latest experimental results⁸⁴ and theoretical calculations of Emmanouilidou and Rost⁸⁵. Reasonable agreements are found with other experimental and theoretical results.

In Fig. 12 we compare our calculated energy resolved double DCS with other available theoretical results^{87,88} for an excess energy (sum of energy of the three ejected electrons) of 115 eV after triple photoionization. The double DCS is given as a function of energy of another outgoing electron by fixing the energy of one electron to be 12.32eV, 28.75 eV, and 53.4 eV, respectively. Colgan *et al.*⁸⁷ calculated energy resolved DCS of triple photoionization of Li using non-perturbative TDCC method. Emmanouilidou⁸⁸ computed double energy resolved DCS in a quasiclassical framework. Note that there is a little difference for the energy of the second electron in the work of Colgan *et al.*⁸⁷ for each case. In the calculation of Colgan *et al.* they chose the photon energy to be 320 eV which corresponds to an excess energy of ~ 120.0 eV. The energy resolved double DCS shows a "U-shape" in all calculations. The larger the excess energy, the more pronounced the unequal energy sharing between the three electrons. A reasonable agreement is found between three theoretical calculations except for Colgan *et al.*⁸⁷ at the lowest and the highest electron energies.

In what follows we would like to say a few words on the interference effects in the multi-electron processes. From the detailed investigations on the typical multielectron processes shown in the above three subsections we conclude that the coherence characteristics is mostly lost in the energy resolved DCS and integral cross section. However, the momenta of the ejected electrons continue to be correlated and could be measured with a very high resolution. If the quantum interference can only be found with a resolution beyond the experimental capability, the quantum features of the processes exist only in the calculation of the cross sections or the reaction rates. The partial loss of coherence of particles due to the environment coupling by Coulomb interaction has experimentally explored by Akoury *et al.*⁴ in the DPI of molecular hydrogen. We suggest that the loss of phases of matter wave for the later ionized electrons (not the first-ionized electron) is a general phenomenon, not only for the multielectron processes discussed in this work but also for those such as in strong field ionization⁸⁹. Liu *et al.*⁸⁹ stated that the first-ionized electron in laser-induced non-sequential multiple ionization either leaves immediately after re-collision or joins the other electrons to form a thermalized complex after a time delay of a few hundred attoseconds. Our study will shed light on the quantum manipulation of many particle processes and systems such as the entangled many-particle states in the quantum computing.

IV. CONCLUSION

In summary, we proposed an accurate and practical theoretical formalism on the correlated dynamical multielectron processes by fully taking into account of the advantage of the coherence characteristics of the bound and continuum electrons in the initial and final states. Detailed expressions are obtained to investigate the energy correlations among the continuum electrons and energy resolved differential and integral cross sections in the electron impact direct double ionization processes according to the separation of KO and SO mechanisms. Extension to the higher order multielectron processes is straight forward by adding the contributions of the following KO and SO processes. The method is firstly applied to the electron impact double ionization processes of the ground terms of C^+ , N^+ , and O^+ . The contributions of different mechanisms including both direct and indirect processes are identified for the first time. Then we employ the method to investigate the direct double and triple Auger decay in the K-shell excited states of C^+ $1s2s^22p^2\ ^2D$ and $\ ^2P$. We nicely explain the recent experimental observation of direct triple Auger decay for the first time and confirmed that the signatures of the resonances found in the triple photoionization of C^+ originates solely from the DTAD process of the K-shell resonant states. The calculated energy correlation among the three continuum electrons in both processes of electron impact double ionization and direct triple Auger decay support a physical scenario of a faster and two slower electrons. At last, the approach is applied to investigate the double and triple photoionization of atomic lithium and comparisons are made with available experimental and theoretical results. Our results show that the proposed approach is accurate and effective in the treatment of atomic multielectron processes. It is natural to extend the present theoretical formalism to the higher more-electron processes. It should also be tractable to extend the present approach to more complex systems such as molecules and clusters.

ACKNOWLEDGMENTS

This work was supported by the National Natural Science Foundation of China under Grant Nos. 11674394 and 11674395.

- ¹V. Shevelko and H. Tawara, *Atomic multielectron processes* (Springer-Verlag Berlin Heidelberg New York, 1998).
- ²G. Tanner, K. Richter, and J. Rost, *Rev. Mod. Phys.* **72**, 497 (2000).
- ³T. Weber, A. O. Czasch, O. Jagutzki, A. K. Müller, V. Mergel, A. Kheifets, E. Rotenberg, G. Meigs, M. H. Prior, S. Daveau, A. Landers, C. L. Cocke, T. Osipov, R. D. Muino, H. Schmidt-Böcking, and R. Dörner, *Nature (London)* **431**, 437 (2004).
- ⁴D. Akoury, K. Kreidi, T. Jahnke, Th. Weber, A. Staudte, M. Schöffler, N. Neumann, J. Titze, L. Ph. H. Schmidt *et al.*, *Science* **318**, 949 (2007).
- ⁵A. Knapp, A. Kheifets, I. Bray, Th. Weber, A. L. Landers, S. Schössler, T. Jahnke, J. Nickles, S. Kammer *et al.*, *Phys. Rev. Lett.* **89**, 033004 (2002).
- ⁶M.S. Schöffler, C. Stuck, M. Waitz, F. Trinter, T. Jahnke, U. Lenz, M. Jones, A. Belkacem, A. L. Landers *et al.*, *Phys. Rev. Lett.* **111**, 013003 (2013).
- ⁷A.H. Liu and U. Thumm, *Phys. Rev. Lett.* **115**, 183002 (2015).
- ⁸A. Lahmam-Bennani, C. Dupre, and A. Duguet, *Phys. Rev. Lett.* **63**, 1582 (1989).
- ⁹M.J. Ford, J.H. Moore, M.A. Coplan, J.W. Cooper, and J.P. Doering, *Phys. Rev. Lett.* **77**, 2650 (1996).
- ¹⁰I. Taouil, A. Lahmam-Bennani, A. Duguet, and L. Avaldi, *Phys. Rev. Lett.* **81**, 4600 (1998).
- ¹¹B. El-Marji, J.P. Doering, J.H. Moore, and M.A. Coplan, *Phys. Rev. Lett.* **83**, 1574 (1999).
- ¹²A. Dorn, A. Kheifets, C.D. Schröter, B. Najjari, C. Höhr, R. Moshhammer, and J. Ullrich, *Phys. Rev. Lett.* **86**, 3755 (2001).
- ¹³R.W. van Boeyen, N. Watanabe, J.P. Doering, J.H. Moore, and M.A. Coplan, *Phys. Rev. Lett.* **92**, 223202 (2004).
- ¹⁴M. Dürr, A. Dorn, J. Ullrich, S.P. Cao, A. Czasch, A.S. Kheifets, J.R. Götz, and J.S. Briggs, *Phys. Rev. Lett.* **98**, 193201 (2007).
- ¹⁵T.A. Carlson, and M.O. Krause, *Phys. Rev. Lett.* **14**, 390 (1965).
- ¹⁶J. Viefhaus, S. Cvejanovic, B. Langer, T. Lischke, G. Prümper, D. Rolles, A. V. Golovin, A. N. Grum-Grzhimailo, N. M. Kabachnik, and U. Becker, *Phys. Rev. Lett.* **92**, 083001 (2004).
- ¹⁷P. Lablanquie, L. Andric, J. Palaudoux, U. Becker, M. Braune, J. Viefhaus, J.H.D. Eland, F. Penent, J. Electron Spectrosc. Relat. Phenom. **156**, 51 (2007).
- ¹⁸Y. Hikosaka, P. Lablanquie, F. Penent, J. Palaudoux, L. Andric, K. Soejima, E. Shigemasa, I.H. Suzuki, M. Nakano, and K. Ito, *Phys. Rev. Lett.* **107**, 113005 (2011).

- ¹⁹C.W. Hogle, X.M. Tong, L. Martin, M.M. Murnane, H.C. Kapteyn, and P. Ranitovic, Phys. Rev. Lett. **115**, 173004 (2015).
- ²⁰J.P. Colgan, and M. S. Pindzola, Phys. Rev. Lett. **108**, 053001 (2012).
- ²¹J.P. Colgan, A. Emmanouilidou, and M. S. Pindzola, Phys. Rev. Lett. **110**, 063001 (2013).
- ²²A. Müller, A. Borovik, Jr., T. Buhr, J. Hellhund, K. Holste, A. L. D. Kilcoyne, S. Klumpp, M. Martins, S. Ricz, J. Viefhaus, and S. Schippers, Phys. Rev. Lett. **114**, 013002 (2015).
- ²³A. Müller *et al.*, J. Phys. Conf. Ser. **635**, 012033 (2015).
- ²⁴P. Lambropoulos, P. Maragakis, and J. Zhang, Phys. Rep. **305**, 203 (1998).
- ²⁵W. Vanroose, F. Martin, T.N. Rescigno, and C.W. McCurdy, Science **310**, 1787 (2005).
- ²⁶H.W. van der Hart and C.H. Greene, Phys. Rev. Lett. **81**, 4333 (1998).
- ²⁷J.P. Colgan, M. S. Pindzola, and F. Robicheaux, Phys. Rev. A **72**, 022727 (2005).
- ²⁸A.Y. Istomin, A. F. Starace, N. L. Manakov, A. V. Meremianin, A. S. Kheifets and Igor Bray, J. Phys. B: At. Mol. Opt. Phys. **39**, L35 (2006).
- ²⁹I.A. Ivanov and A.S. Kheifets, Phys. Rev. A **85**, 013406 (2012).
- ³⁰P. Singh, G. Purohit, A. Dorn, X.G. Ren and V. Patidar, J. Phys. B: At. Mol. Opt. Phys. **49**, 025201 (2015).
- ³¹I. Bray, Phys. Rev. Lett. **89**, 273201 (2002).
- ³²A.S. Kheifets and I. Bray, Phys. Rev. Lett. **81**, 4588 (1998).
- ³³A. Dorn, A. Kheifets, C.D. Schröter, B. Najjari, C. Höhr, R. Moshhammer, and J. Ullrich, Phys. Rev. A **65**, 032709 (2002).
- ³⁴M.S. Pindzola, J.A. Ludlow, C.P. Ballance, F. Robicheaux and J.P. Colgan, J. Phys. B: At. Mol. Opt. Phys. **43**, 105201 (2010).
- ³⁵M.S. Mengoue, M.G. Kwato Njock, B. Piraux, Yu. V. Popov, and S.A. Zaytsev, Phys. Rev. A **83**, 052708 (2011).
- ³⁶C. Li, A. Lahmam-Bennani, E. M. S. Casagrande and C. D. Cappello, J. Phys. B: At. Mol. Opt. Phys. **44**, 115201 (2011).
- ³⁷M.Ya. Amusia, I.S. Lee, and V.A. Kilin, Phys. Rev. A **45**, 4576 (1992).
- ³⁸M.S. Pindzola, F. Robicheaux, and J.P. Colgan, Phys. Rev. A **72**, 022709 (2005).
- ³⁹M.S. Pindzola, F. Robicheaux, and J.P. Colgan, Phys. Rev. A **73**, 062720 (2006).
- ⁴⁰J. Berakdar, A. Lahmam-Bennani, and C. Dal Cappello, Phys. Rep. **374**, 91 (2003).
- ⁴¹J. Hozzowska, A. K. Kheifets, J.-Cl. Dousse, M. Berset, I. Bray, W. Cao, K. Fennane, Y. Kayser, M. Kavčić, J. Szlachetko, and M. Szlachetko, Phys. Rev. Lett. **102**, 073006 (2009).
- ⁴²S. Huotari, K. Hämäläinen, R. Diamant, R. Sharon, C.C. Kao, and M. Deutsch, Phys. Rev. Lett. **101**, 043001 (2008).
- ⁴³T. Schneider, P.L. Chocian, and J.M. Rost, Phys. Rev. Lett. **89**, 073002 (2002).
- ⁴⁴T. Pattard and J. Burgdörfer, Phys. Rev. A **64**, 042720 (2001).
- ⁴⁵J.L. Zeng, P.F. Liu, W.J. Xiang and J.M. Yuan, Phys. Rev. A **87**, 033419 (2013).
- ⁴⁶J.L. Zeng, P.F. Liu, W.J. Xiang and J.M. Yuan, J. Phys. B: At. Mol. Opt. Phys. **46**, 215002 (2013).
- ⁴⁷P.F. Liu, Y.P. Liu, J.L. Zeng and J.M. Yuan, Eur. Phys. J. D **68**, 214 (2014).
- ⁴⁸M.F. Gu, Can. J. Phys. **86**, 675 (2008).
- ⁴⁹K.A. Berrington, B. W.Eissner, and P.H. Norrington, Comput. Phys. Commun. **92**, 290 (1995).
- ⁵⁰Y.P. Liu, C. Gao, J.L. Zeng, J.M. Yuan, and J. R. Shi, Astrophys. J. Suppl. Series **211**, 30 (2014).
- ⁵¹Y.P. Liu, C. Gao, J.L. Zeng, and J.R. Shi, Astron. Astrophys. **536**, A51 (2011).
- ⁵²Y.P. Liu, J.L. Zeng, and J.M. Yuan, J. Phys. B: At. Mol. Opt. Phys. **46**, 145002 (2013).
- ⁵³J.L. Zeng, L.P. Liu, P.F. Liu, and J.M. Yuan, Phys. Rev. A **90**, 044701 (2014).
- ⁵⁴P.F. Liu, Y.P. Liu, J.L. Zeng and J.M. Yuan, Phys. Rev. A **89**, 042704 (2014).
- ⁵⁵P.F. Liu, J.L. Zeng, Jr. A. Borovik, S. Schippers and A. Müller, Phys. Rev. A **92**, 012701 (2015).
- ⁵⁶J.L. Zeng and J.M. Yuan, Phys. Rev. E **76**, 026401 (2007).
- ⁵⁷J.L. Zeng and J.M. Yuan, Phys. Rev. E **74**, 025401(R) (2006).
- ⁵⁸I.B. Abdurakhmanov, A.S. Kadyrov and I. Bray, J. Phys. B: At. Mol. Opt. Phys. **49**, 03LT01 (2016).
- ⁵⁹M. Lepers, G. Quéméner, E. Luc-Koenig and O. Dulieu, J. Phys. B: At. Mol. Opt. Phys. **49**, 014004 (2016).
- ⁶⁰X.G. Ren, A. Dorn, and J. Ullrich, Phys. Rev. Lett. **101**, 093201 (2008).
- ⁶¹G. Gasaneo, D.M. Mitnik, J.M. Randazzo, L.U. Ancarani, and F.D. Colavecchia, Phys. Rev. A **87**, 042707 (2013).
- ⁶²M.S. Pindzola, F.J. Robicheaux, J.P. Colgan, M.C. Witthoef, and J.A. Ludlow, Phys. Rev. A **70**, 032705 (2004).
- ⁶³M.S. Pindzola, F. Robicheaux, and J.P. Colgan, Phys. Rev. A **76**, 024704 (2007).
- ⁶⁴M.S. Pindzola, J.A. Ludlow, C.P. Ballance, F. Robicheaux, and J.P. Colgan, J. Phys. B: At. Mol. Opt. Phys. **44**, 105202 (2011).
- ⁶⁵M.S. Pindzola, J.A. Ludlow, F. Robicheaux, J.P. Colgan, and D.C. Griffin, J. Phys. B: At. Mol. Opt. Phys. **42**, 215204 (2009).
- ⁶⁶M. Zambra, D. Belic, P. Defrance, and D.J. Yu, J. Phys. B: At. Mol. Opt. Phys. **27**, 2383 (1994).
- ⁶⁷M. Westermann, K. Aichele, U. Hartenfeller, D. Hathiramani, M. Steidl, and E. Salzborn, Phys. Scr. **T80**, 285 (1999).
- ⁶⁸J. Lecointre, K.A. Kouzakov, D.S. Belic, P. Defrance, Yu.V. Popov, and V.P. Shevelko, J. Phys. B: At. Mol. Opt. Phys. **46**, 205201 (2013).
- ⁶⁹V. Jonauskas, A. Pranciševičius, S. Masys, and A. Kyniene, Phys. Rev. A **89**, 052714 (2014).

- ⁷⁰Y. Ralchenko, A. Kramida, J. Reader, and NIST ASD Team, Atomic Spectra Database (Gaithersburgh, MD: NIST), <http://physics.nist.gov/asd>.
- ⁷¹F.Y. Zhou, Y.L. Ma, and Y.Z. Qu, Phys. Rev. A **93**, 060501(R) (2016).
- ⁷²J.A.R. Samson, W.C. Stolte, Z.X. He, J.N. Cutler, Y. Lu, and R.J. Bartlett, Phys. Rev. A **57**, 1906 (1998).
- ⁷³K.I. Hino, T. Ishihara, F. Shimizu, N. Toshima, and J.H. McGuire, Phys. Rev. A **48**, 1271 (1993).
- ⁷⁴J.P. Colgan, D.C. Griffin, C.P. Ballance, and M. S. Pindzola, Phys. Rev. A **80**, 063414 (2009).
- ⁷⁵H.W. van der Hart, and C.H. Greene, Phys. Rev. Lett. **81**, 4333 (1998).
- ⁷⁶A.S. Kheifets, D.V. Fursa and I. Bray, Phys. Rev. A **80**, 063413 (2009).
- ⁷⁷R. Wehlitz, J.P. Colgan, M. M. Martinez, J. B. Bluett, D. Lukić, and S. B. Whitfield, Journal of Electron Spectroscopy and Related Phenomena **144-147**, 59 (2005).
- ⁷⁸M.T. Huang, R. Wehlitz, Y. Azuma, L. Pibida, I.A. Sellin, J.W. Cooper, M. Koide, H. Ishijima, and T. Nagata, Phys. Rev. A **59**, 3397 (1999).
- ⁷⁹R. Wehlitz, J.B. Bluett, and S.B. Whitfield, Phys. Rev. A **66**, 012701 (2002).
- ⁸⁰A.I. Mikhailov, A.V. Nefiodov, and G. Plunien, Phys. Lett. A **375**, 823 (2011).
- ⁸¹J.P. Santos, M.F. Laranjeira and F. Parente, Europhys. Lett. **55**, 479 (2001).
- ⁸²R. Wehlitz, T. Pattard, M.T. Huang, I.A. Sellin, J. Burgdörfer, and Y. Azuma, Phys. Rev. A **61**, 030704(R) (2000).
- ⁸³T. Pattard, and J. Burgdörfer, Phys. Rev. A **63**, 020701(R) (2001).
- ⁸⁴P.N. Juranić, and R. Wehlitz, Phys. Rev. A **78**, 033401 (2008).
- ⁸⁵A. Emmanouilidou, and J. M. Rost, J. Phys. B: At. Mol. Opt. Phys **39**, L99 (2006).
- ⁸⁶R. Wehlitz, M.T. Huang, B.D. Depaola, J.C. Levin, I.A. Sellin, T. Nagata, J.W. Cooper, and Y. Azuma, Phys. Rev. Lett. **81**, 1813 (1998).
- ⁸⁷J.P. Colgan, and M. S. Pindzola, J. Phys. B: At. Mol. Opt. Phys **39**, 1879 (2006).
- ⁸⁸A. Emmanouilidou, Phys. Rev. A **75**, 042702 (2007).
- ⁸⁹X. Liu, C. Figueira de Morisson Faria and W. Becker, New Journal of Physics **10**, 025010 (2008).

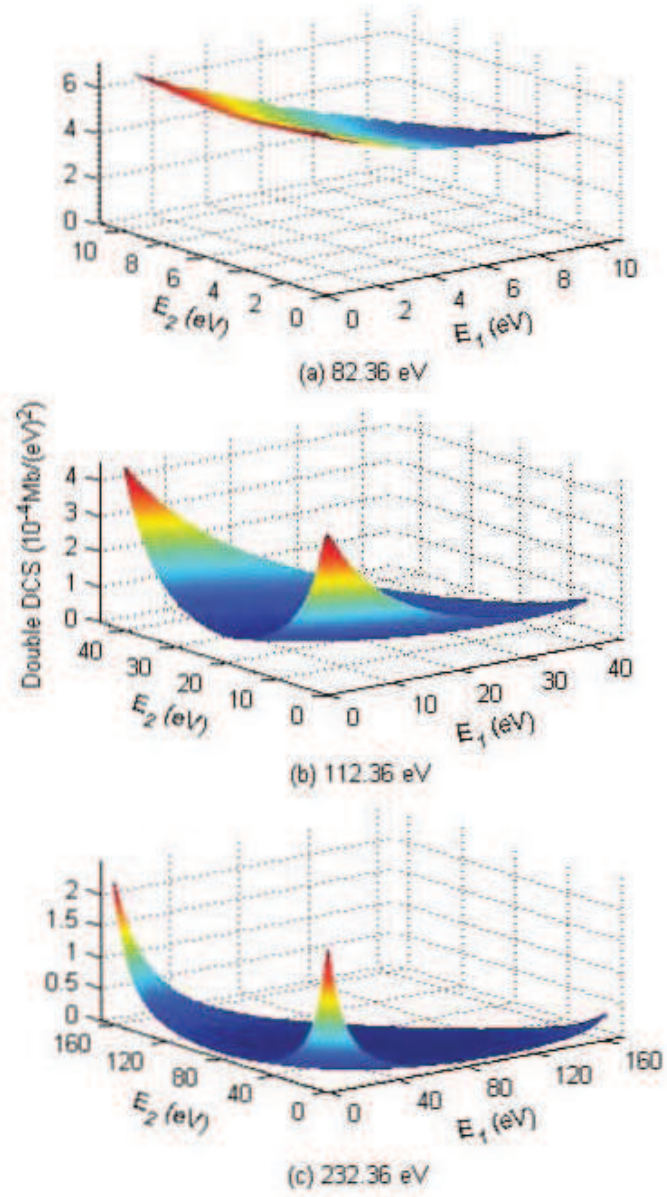


FIG. 4. Energy resolved double differential cross section (DCS) of the ground term of C^+ at incident electron energies of (a) 82.36 eV, (b) 112.36 eV and (c) 232.36 eV, which are above the double ionization threshold by 10.0, 40.0, and 160.0 eV, respectively, for the pathway of $e+C^+ 1s^2 2s^2 2p^2 P^o \rightarrow C^{2+} 1s^2 2s^2 ^1S + 2e \rightarrow C^{3+} 1s^2 2s^2 S + 3e$ in the electron impact direct double ionization process.

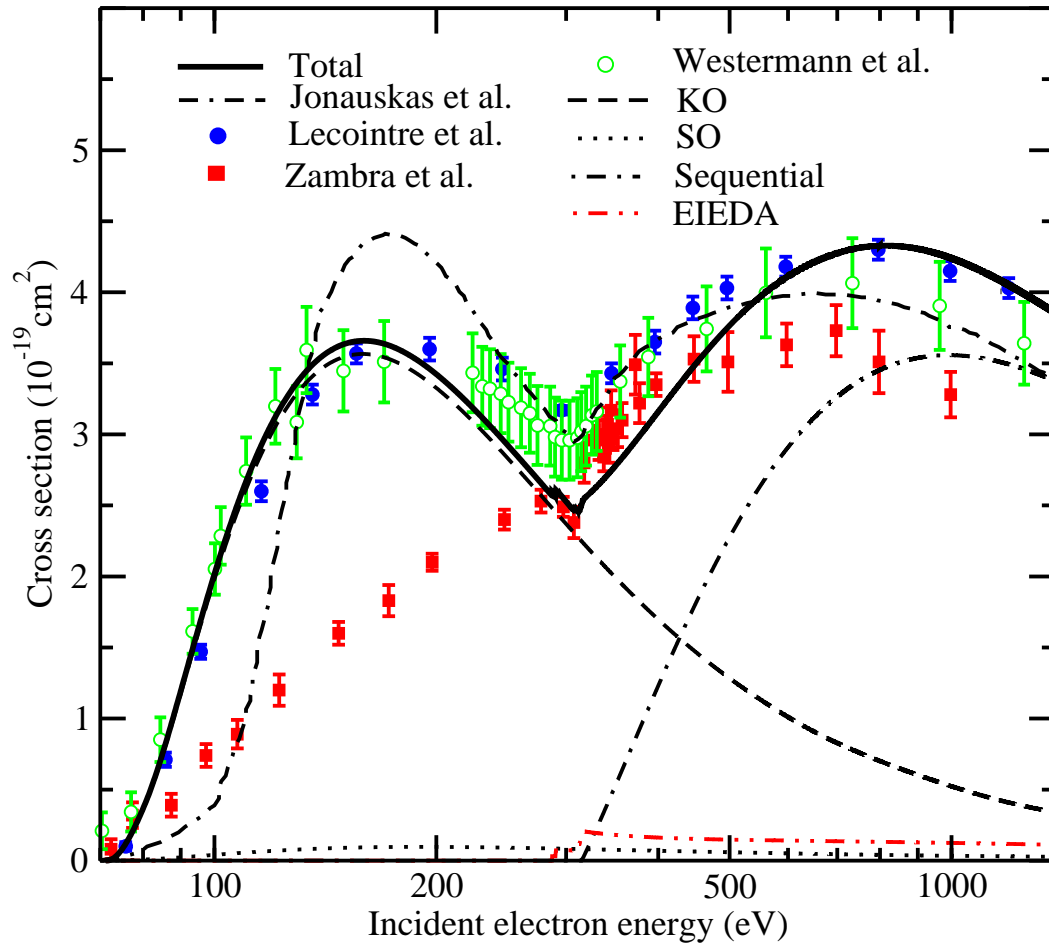


FIG. 5. Comparison of theoretical electron impact double ionization cross section (the solid line) of the ground term of C^+ with the experimental⁶⁶⁻⁶⁸ and theoretical results⁶⁹. The direct double ionization cross section contributed by KO and SO mechanisms and indirect processes of sequential and electron impact excitation double autoionization (EIEDA) are given separately to evaluate their relative importance.

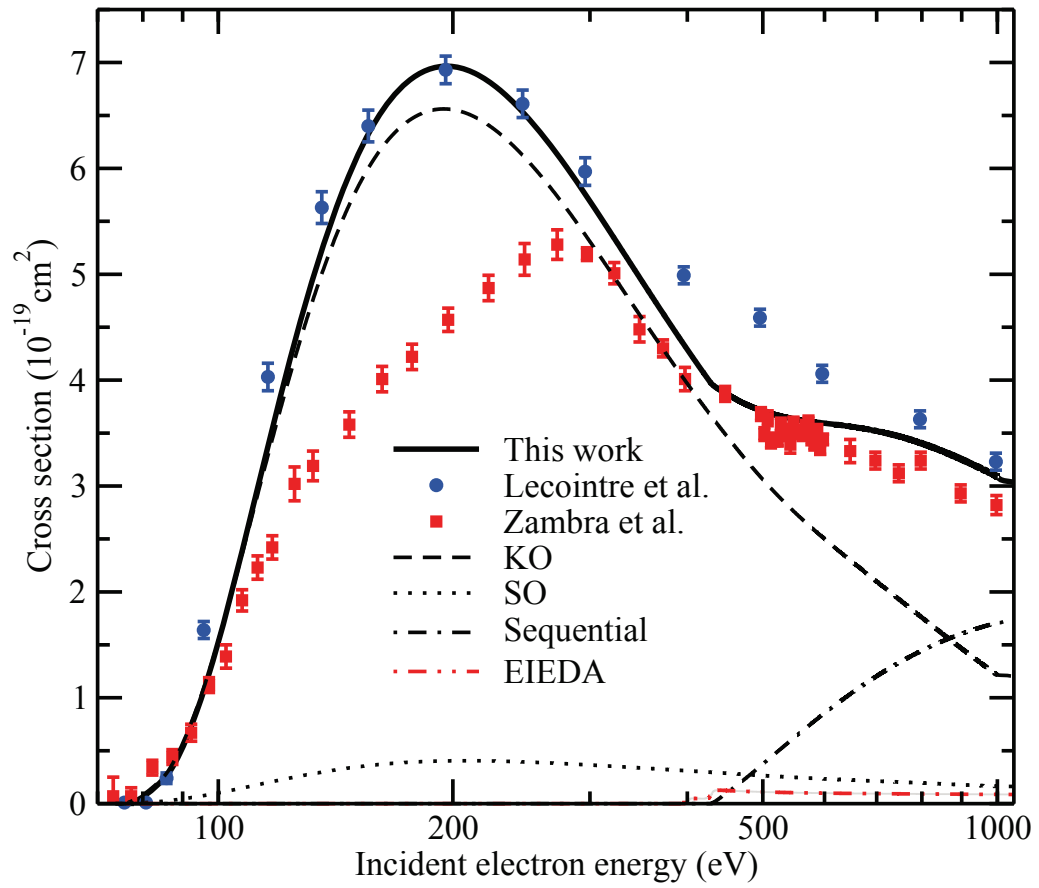


FIG. 6. As in Fig. 5 but for the electron impact double ionization of the ground term of N^+ .

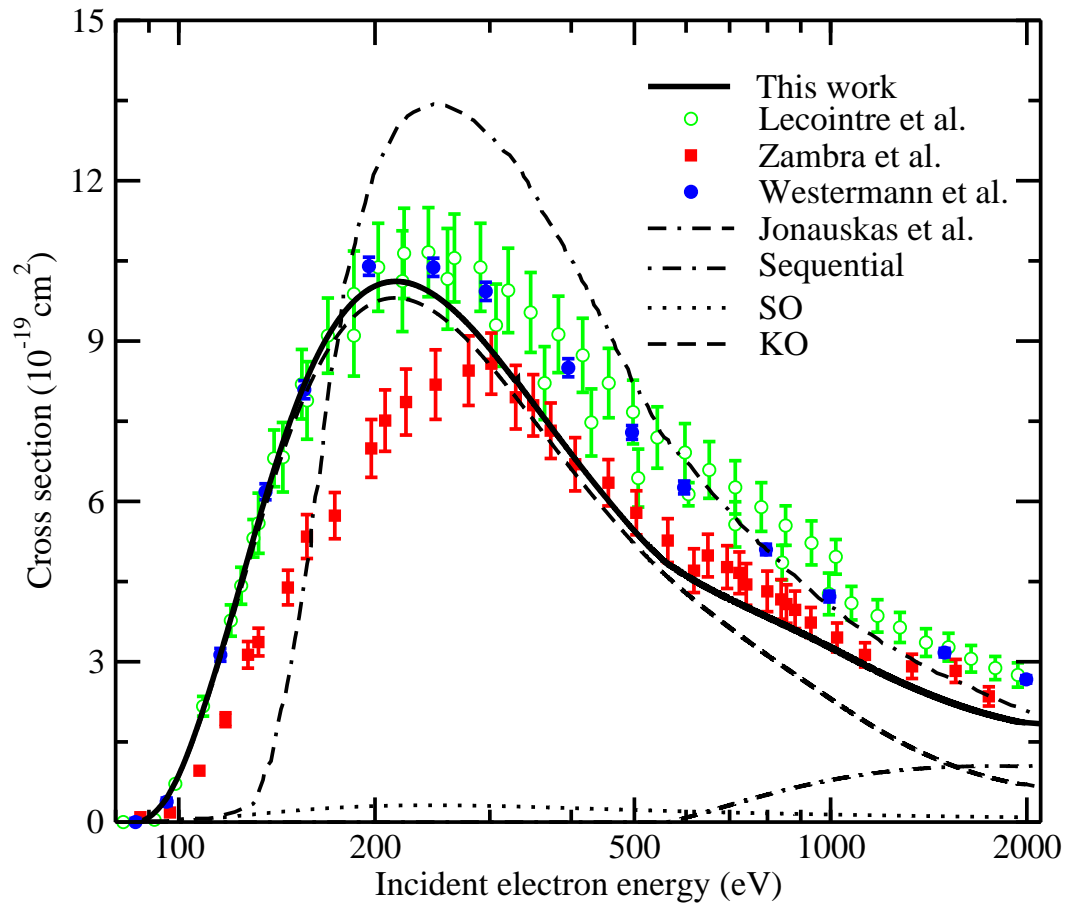


FIG. 7. As in Fig. 5 but for the electron impact double ionization of the ground term of O^+ .

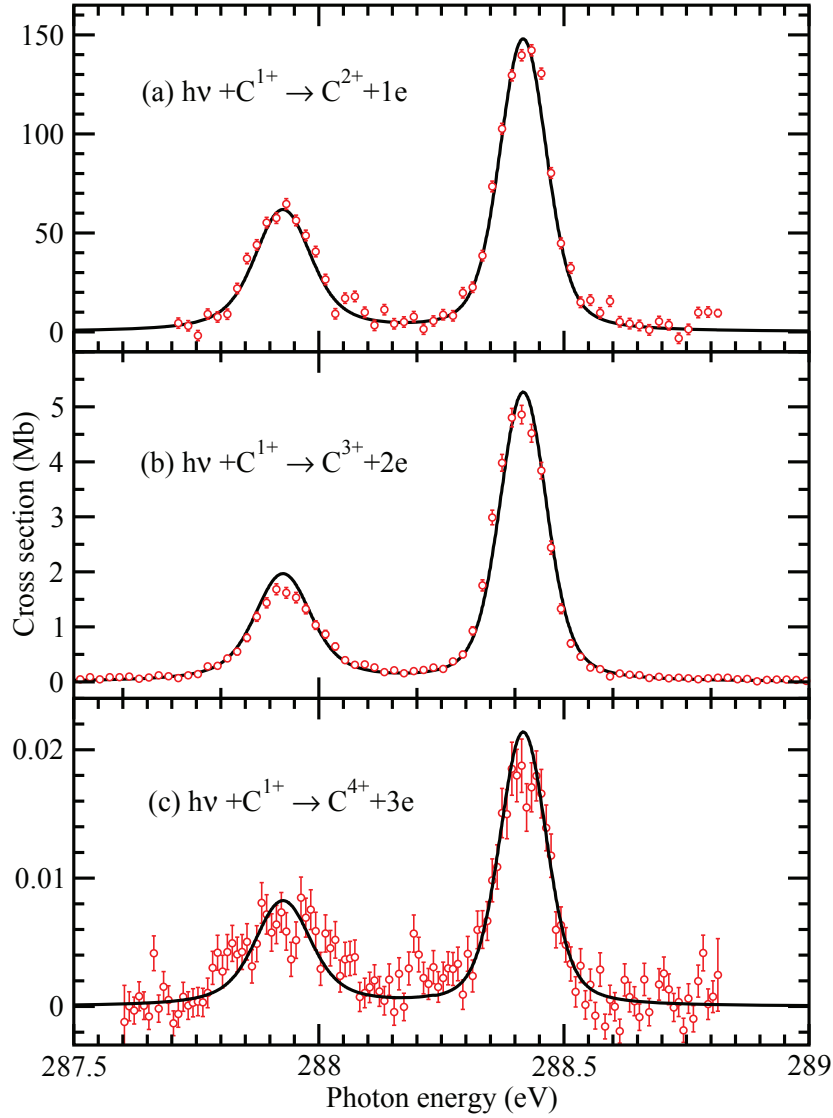


FIG. 8. Comparison of theoretical (this work, solid line) and experimental (open circles with error bars)²² cross sections for the single (a), double (b), and triple (c) ionization of C^+ ions by a single photon near the K-shell resonances of $1s2s^22p^2\ ^2D$ and $\ ^2P$. The instrument bandwidth of 92 meV in the experiment has been included in the theoretical results. To have a better comparison, we have shifted the resonance positions toward lower photon energy direction by 0.6 eV and 0.7 eV for $\ ^2D$ and $\ ^2P$ terms, respectively.

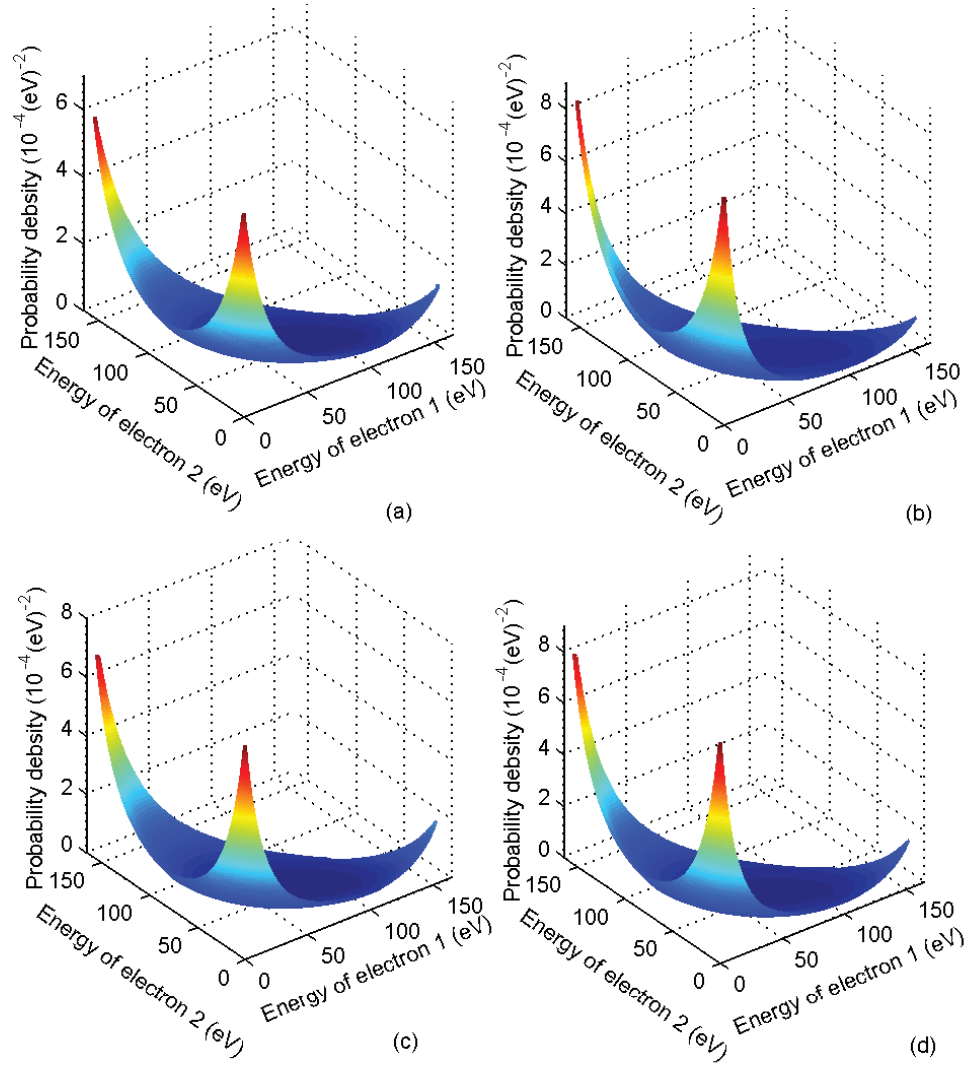


FIG. 9. Total probability density as a function of energies of two continuum electrons in the DTAD processes of $C^+ 1s2s^22p^2\ ^2D$ term for the four strongest pathways: (a) $C^{2+} 1s^22s^2\ ^1S \rightarrow C^{3+} 1s^22s^2\ ^2S \rightarrow C^{4+} 1s^2$, (b) $C^{2+} 1s^22s2p\ ^1P^o \rightarrow C^{3+} 1s^22s^2\ ^2S \rightarrow C^{4+} 1s^2$, (c) $C^{2+} 1s^22s2p\ ^1P^o \rightarrow C^{3+} 1s^22p^2\ ^2P^o \rightarrow C^{4+} 1s^2$, and (d) $C^{2+} 1s^22s^02p^2\ ^1D \rightarrow C^{3+} 1s^22p^2\ ^2P^o \rightarrow C^{4+} 1s^2$.

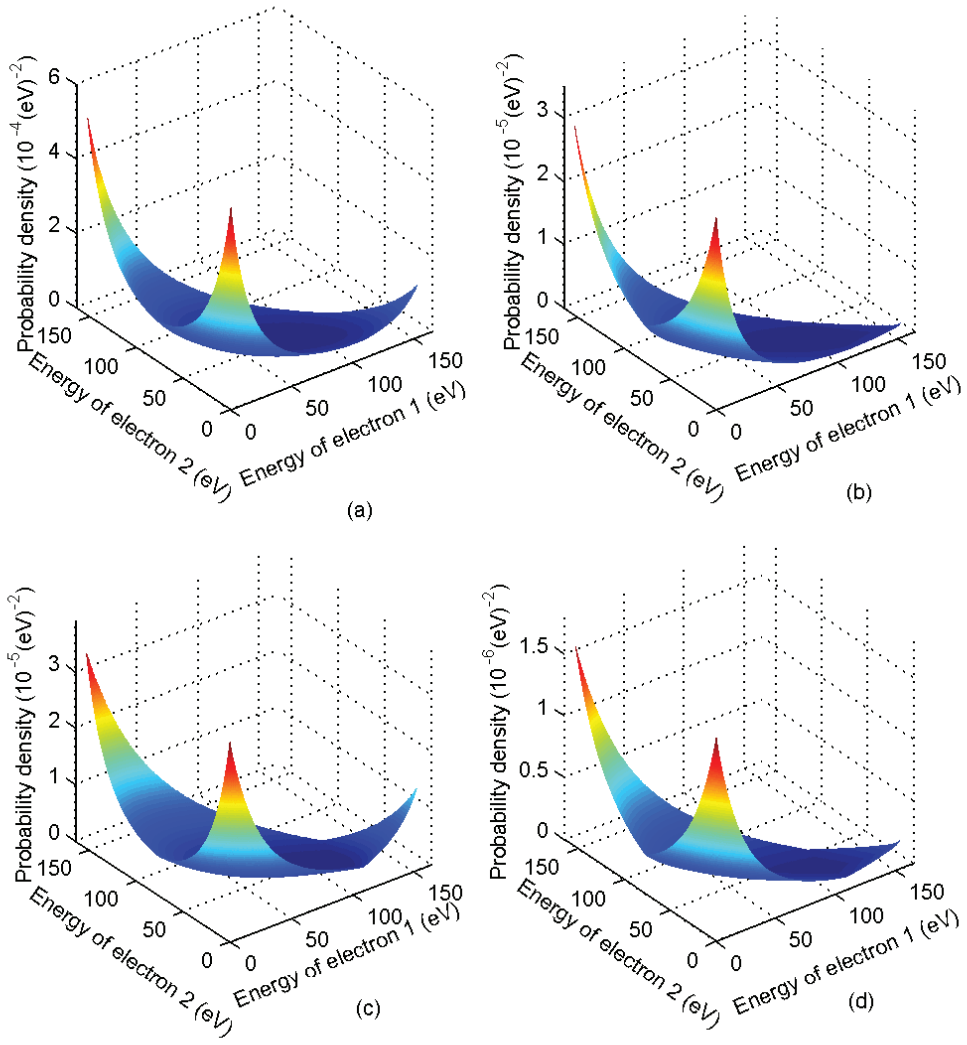


FIG. 10. Probability density contributed by (a) double KO, (b) KO+SO, (c) SO+KO, and (d) double SO for the pathway of $C^+ 1s2s^2 2p^2 \ ^2D \rightarrow C^{2+} 1s^2 2s^2 \ ^1S \rightarrow C^{3+} 1s^2 2s \ ^2S \rightarrow C^{4+} 1s^2$.

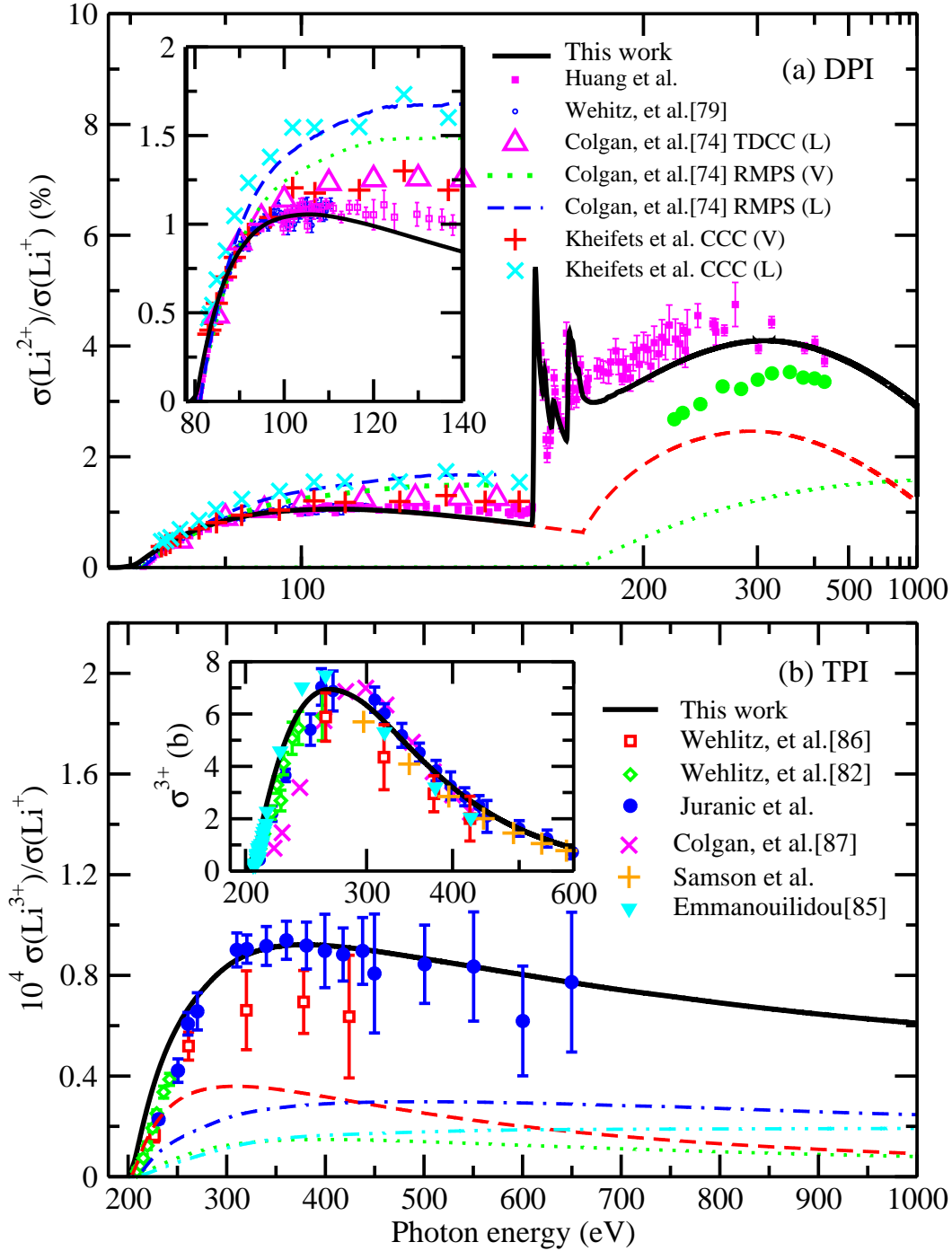


FIG. 11. (a) Double-to-single ratio of photoionization cross section for atomic lithium compared with available experimental^{78,79} and theoretical results of the length and velocity gauges of CCC calculations by Kheifets *et al.*⁷⁶ and the length gauge of TDCC, length and velocity gauges of RMPS by Colgan *et al.*⁷⁴ available in the literature. The calculations of CCC(L), CCC(V), TDCC (L), RMPS(L), and RMPS(L) are represented by \times , +, magenta \triangle , a blue dashed line, and a green dotted line, respectively. The dashed and dotted lines represent the cross section contributed by the KO and SO mechanisms. The inset enlarged the double-to-single ratio from the ionization threshold to a photon energy of 140 eV to have a better comparison near the double ionization threshold. (b) Comparison of our theoretical triple-to-single ratio of photoionization cross section of lithium with available experimental measurements by Wehitz *et al.*^{82,86} and Juranić *et al.*⁸⁴ and theoretical results of Colgan *et al.* (magenta \times)²⁷, Emmanouilidou and Rost (cyan ∇)⁸⁵, and Samson *et al.*⁷² (yellow +). The cross section contributed by the KO+KO, KO+SO, SO+KO, and SO+SO mechanisms are represented by a red dashed, blue dotted-dashed, dotted-dotted-dashed, and green dotted line, respectively. In the inset, a comparison is made for the triple photoionization cross section with available experimental and theoretical results.

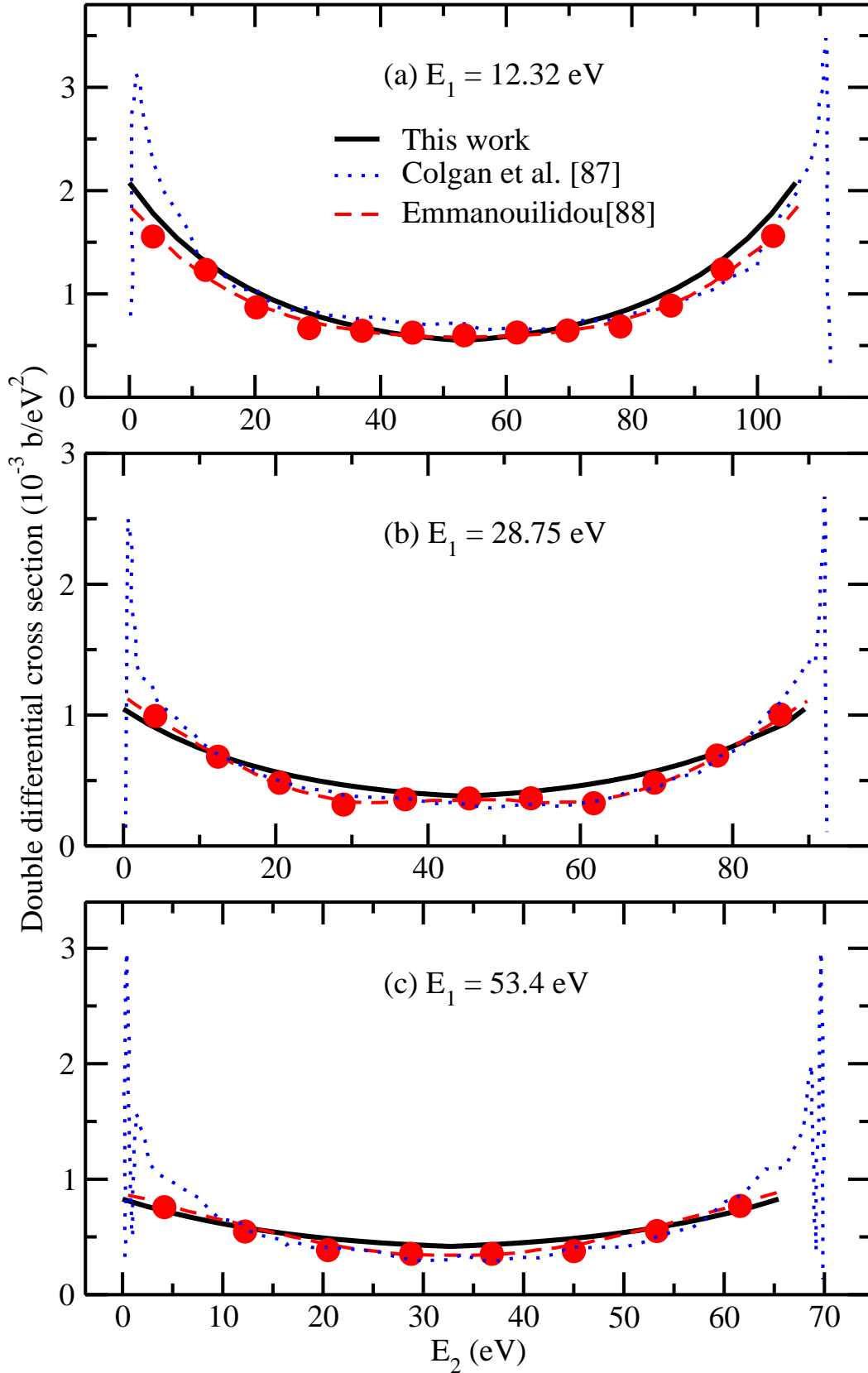


FIG. 12. Energy resolved double DCS for triple photoionization of the ground state of atomic Li at an excess energy of 115 eV. By fixing the energy of one electron to be (a) 12.32 eV, (b) 28.75 eV, (c) 53.4 eV, we show the double DCS as a function of the energy of another continuum electron. Red circles and red lines represent the theoretical calculations in a quasiclassical framework⁸⁸ and blue dotted lines are the theoretical results from Ref.⁸⁷ at a photon energy of 320 eV.